Achieving optimum hydrogen permeability in PdAg and PdAu alloys

Chandrashekhar G. Sonwane, Jennifer Wilcox,[a] and Yi Hua Ma
Department of Chemical Engineering, Worcester Polytechnic Institute, Worcester, Massachusetts 01609

(Received 26 July 2006; accepted 6 October 2006; published online 14 November 2006)

The present work investigates both the diffusivity and permeability of hydrogen (H) in palladium-silver (PdAg) and palladium-gold (PdAu) alloys over a 400–1200 K temperature range for $Pd_{100-X}M_X$, M=Ag or Au and X=0%–48% using density functional theory (DFT) and kinetic Monte Carlo simulations (KMC). DFT has been employed to obtain octahedral (O)-, tetrahedral (T)-, and transition state (TS)- site energetics as a function of local alloy composition for several PdAg and PdAu alloys with compositions in supercells of X=14.18%, 25.93%, 37.07%, and 48.15% with the nearest (NNs) and next nearest neighbors (NNNs) varied over the entire range of compositions. The estimates were then used to obtain a model relating the O, T, and TS energies of a given site with NN_X, NNN_X, and the lattice constant. The first passage approach combined with KMC simulations was used for the H diffusion coefficient predictions. It was found that the diffusion coefficient of H in PdAg alloy decreases with increasing Ag and increases with increasing temperature, matching closely with the experimental results reported in the literature. The calculated permeabilities of H in these novel binary alloys obtained from both diffusivity and solubility predictions were found to have a maximum at ~20% Ag and ~12% Au, which agree well with experimental predictions. Specifically, the permeability of H in PdAg alloy with ~20% Ag at 456 K is three to four times that of pure Pd, while the PdAu alloy at 12% Au is four to five times that of pure Pd at 456 K. © *2006 American Institute of Physics*. [DOI: 10.1063/1.2387166]

I. INTRODUCTION

From an environmental standpoint, high purity hydrogen appears to be an ideal fuel source. Contribution to both the greenhouse effect and urban pollution can be reduced by using cleaner energy based upon this renewable source. For the last 150 years, the trend in energy use has been toward reducing carbon consumption and increasing the use of hydrogen. The present and future applications of hydrogen include powering nonpolluting vehicles, heating homes and offices, fueling aircrafts, ammonia manufacture, methanol synthesis, fuel for space shuttles, and fuel cells that provide heat and electricity and drinking water for astronauts. However, widespread use will require cheaper means of producing hydrogen, safer ways to store it, and new means to distribute hydrogen from the producer to the end user and fueling stations.

One of the important ways of producing high purity hydrogen is through the catalytic reaction of steam with hydrocarbons or coke and then separating the hydrogen from the mixtures using palladium-based membranes. The cost of producing hydrogen can be reduced by the fabrication of very thin, high-permeability Pd-based membranes that are stable at high temperature and pressures and for the long operation times typically employed in petrochemical industries.

The operating lifetime of pure Pd membranes is low since, during the absorption and desorption cycles of H while operating below the critical temperature, the structure of Pd undergoes expansions and contractions due to $\alpha \leftrightarrow \beta$ phase transformations,[1] leading to the formation of cracks from embrittlement. Several experimental reports suggest that alloying Pd with other metals such as Ag, Au, or Cu helps by reducing potential embrittlement, offering resistance to poisoning, and providing a longer operational lifetime, which are important for reducing the cost of producing H. The PdCu alloy has been found to be tolerant to sulfur poisoning;[2–4] however, it has significantly lower H permeability as compared to pure Pd. The first experimental investigation suggesting the higher solubility of H in PdAg alloy as compared to pure Pd was performed by Graham[5] in 1869. In another pioneering effort, Gryaznov[6] reported that the permeability of H in PdAg is higher than in pure Pd. Experiments in the past have shown that, either at ~20% (Ref. 7) or between 23% and 32%,[8] Ag in a PdAg alloy has significantly higher permeability as compared to pure Pd. The addition of Ag reduces the critical temperature of $\alpha \leftrightarrow \beta$ phase transformations and also increases the solubility of H, while simultaneously reducing its diffusion coefficient, causing an increased H permeability. In addition, Gryaznov[6] found that alloying Pd with Au yields a H permeability 2.2 times that of pure Pd at a 10% Au content. Amandusson *et al.*[9] found that PdAg alloy with 32% Ag at 623 K has six times higher permeability as compared to pure Pd. In addition, PdAg alloy with compositions greater than 30% Ag does not have $\alpha \leftrightarrow \beta$ phase transformations occurring at low temperatures, which is a major cause of defects in membranes. The addition of Cu

[a]Fax: 508-831-5853. Electronic mail: jwilcox@wpi.edu

causes the contraction of the Pd cell while the addition of Ag or Au causes cell expansion. It has been hypothesized that by providing an expanded lattice, i.e., PdAg or PdAu, one can avoid the expansion/contractions, thereby reducing the embrittlement of the membrane due to limiting the $\alpha \leftrightarrow \beta$ phase transformations.[9] However, this is a debatable issue which will be discussed in this manuscript. By changing the alloy composition, the solubility and diffusion coefficient can be adjusted to obtain maximum permeation.

Specifically, there have been no *ab initio* based simulations reported in the literature describing the permeability of H in PdAg and PdAu. There have been several simulation-based studies that provide qualitative explanation of higher H solubility in PdAg alloy based on the adjacent Ag atoms, but no quantitative estimates of solubility, permeability, or diffusion coefficient predictions have ever been reported. Similarly, to the authors' knowledge, there are no simulation studies discussing solubility, diffusion coefficient, and permeability of H in PdAu alloys. The density functional theory (DFT) based simulation studies with PdAg alloy reported in the literature fail to account for the random arrangement of varying octahedral (O)-and tetrahedral (T)-site energies and the effect of local alloy composition. Instead, these approaches use the approximation of representing the PdAg alloy as a cluster of four atoms in an fcc arrangement (providing four distinct alloying compositions, 0%, 25%, 50%, 75%, and 100% Ag in PdAg alloy) with or without periodic boundary conditions. The system and approach used by these researchers[10–12] do not provide the flexibility of estimating the binding energy as well as solubility of PdAg and PdAu alloys with intermediate alloy compositions, hydrogen concentrations, and operating conditions (temperature, pressure) in order to find a suitable system composition and operating conditions for higher permeability. We have also considered the effect of lattice expansion due to H on the permeability which is completely ignored under the assumption that they are negligible. Although there have been attempts to estimate the absorption energy to use as a tool to provide a qualitative trend in solubility, there have been no attempts to predict the solubility, diffusion coefficient, or permeability of PdAg or PdAu alloys by *ab initio* simulations against experimental data. This study is expected to lead experimentalists to the design efficient membranes at the desired operating conditions. The main goals of the present work involve the theoretical prediction of the solubility, diffusion coefficient, and permeability of H in PdAg and PdAu systems and comparing them with the experimental data available in the literature.

II. THEORETICAL METHODOLOGY

A. O-, T-, and TS-site energetics

All the alloys were simulated as three dimensional infinite periodic structures by defining a supercell with atoms on an fcc lattice with periodic boundary conditions in all three principal axes. The Vienna *ab initio* simulation package (VASP) was used for all the simulations.[13,14] The electron exchange correlation effects were described by a generalized gradient approximation (GGA) using the Perdew-Wang 91 functional. A plane wave expansion with a cutoff of 199 eV was used in all of the calculations for Pd, PdAg, and PdAu alloys. The total energy calculations used the residual minimization method for electronic relaxation, and the calculations were accelerated using the Methfessel-Paxton Fermi-level smearing with a width of 0.2 eV. Geometry relaxation calculations employed the conjugate-gradient (CG) algorithm until the forces on the unconstrained atoms were less than 0.03 eV/Å. A Monkhorst-Pack mesh with a $4\times4\times4$ k grid was used for all the simulations involving Pd, PdAg, and PdAu alloys.

In the present work, we have estimated the binding energy of O and T sites using (1),

$$E_x = E_{\mathrm{Pd}M+\mathrm{H}} - E_{\mathrm{Pd}M} - \tfrac{1}{2}E_{\mathrm{H}_2}, \tag{1}$$

where x represents either O or T.

The method of simulating H diffusion in Pd-based alloys is more complex than that of pure Pd. The first step is to simulate an accurate structure of a given Pd alloy with regard to the relative arrangement of Pd and Ag (or Au) atoms in the lattice and the type of crystal lattice from which these atoms are distributed. The information of the crystal lattice can be obtained from the phase diagrams available in the literature.[15] In the present work, the PdAg and PdAu systems were modeled as completely miscible fcc crystal structures. The phase diagram of PdAg (Ref. 15) is a continuous miscible PdAg structure over the entire composition and temperature range considered. The PdAu system[15] is a miscible fcc structure except for a narrow range of composition and temperature. Specifically, between 13%–30% and 70%–80% of Pd in PdAu alloy (in 873–1073 K) and 43%–55% Pd (in 293–363 K) in PdAu alloy may have a cubic or other unknown structure (not fcc). However, due to the uncertainty in knowing the details of the structure at these different composition/temperature conditions, a uniform approach involving strictly fcc structures had to be considered in the present work. In the present work, for the simulation of solubility, a structure with 6234 atoms has been used. Through a comparison to larger-volume simulations it was verified that this number of atoms was sufficient to yield results not affected by finite-size effects. A supercell with 27 atoms was used to estimate the dependence of binding energy on the nearest neighbors, next nearest neighbors, and lattice constant. Supercells with a larger number of atoms were also considered, yielding a minimal change in energetic predictions, so that, to optimize computational cost and efficiency, the 27-atom system was chosen for the simulations. For each alloy composition, the position of Pd and Ag atoms was changed such that several combinations of nearest neighbors (NNs) (minimum of 0, maximum of 6) and next nearest neighbors (NNNs) (minimum of 0, maximum of 8) referring to the number of Ag (or Au) atoms were assumed. Alloy compositions of $\mathrm{Pd}_{100-x}\mathrm{Ag}_x$ with $x=14.81$, 25.93, 37.04, and

48.51, $Pd_{100-x}Au_x$ with $x=14.81$, 25.93, and 37.04, and $Pd_{100-x}Cu_x$ with $x=25.93$ and 48.51 were considered. A nonlinear equation was used to obtain a predicted binding energy with NN, NNN, and lattice constant as independent variables.

The solubility was estimated using $\theta=K_S P_{H_2}^{1/2}$ where, θ is the solubility, K_S is Sievert's constant, and P_{H_2} is the H pressure in the gas phase. Sievert's constant was estimated using Eq. (2),[16,17]

$$K_S = \exp\left(\beta\left[-\frac{D_E}{2}+\frac{h\nu_{H_2}}{4}-E_O-\frac{3}{2}h\nu_H\right]\right) \times\frac{1}{\sqrt{\alpha}}\sqrt{1-\exp(-\beta h\nu_{H_2}/2)}\frac{1}{(1-e^{-\beta h\nu_H})}, \quad (2)$$

where

$$\alpha=\left(\frac{2\pi mkT}{h^2}\right)^{3/2}\frac{4\pi^2 I(kT)^2}{h^2} \quad (3)$$

and $\beta=1/k_BT$, k_B is Boltzmann's constant, D_E is the classical dissociation energy, E_O is the binding energy, h is Planck's constant, I is the molecular moment of inertia, ν_H and ν_{H_2} are vibrational frequencies of H in the Pd and gaseous states, respectively, m is the mass of the H molecule.

B. Activation energy and diffusion coefficient

The permeation of hydrogen in PdAg and PdAu alloys is described by a hopping mechanism that occurs between the adjacent interstitial sites, with each hop having an activation energy that can be used in conjunction with transition state theory (TST) to determine a rate constant for that particular hop. The rate constant for each hop depends upon the type of hop, i.e., T-O or O-T, and the energy of the individual sites, i.e., E_O, E_T and E_{TST}. The energy of the individual binding energies at the O site (E_O) and T site (E_T) were estimated as described earlier. For E_{TS}, the Lanczos algorithm has been applied.[18,19] In this method, the configuration is pushed along a random direction with a given step size until a negative eigenvalue appears. The procedure is repeated until the lowest eigenvalue passes a threshold, at which the configuration is moved to a saddle point by moving along the eigenvector corresponding to this value. If the lowest eigenvalue changes sign, the iterative procedure is stopped and a new event begins. The Lanczos algorithm works by iteratively projecting a vector upon the Hamiltonian. A Monkhorst-Pack mesh with a $4\times4\times4$ k grid was used for all the simulations. The transition state energy (E_{TS}) obtained was then studied using a model that was then incorporated into a KMC algorithm. It was assumed that the activation energy required for each hop was dependent upon the local alloy composition with atoms in the NN and NNN shell (the atoms surrounding the adjacent O site) as well as the lattice constant. The zero-point energies (ZPE) in the present work were estimated for several individual O, T, and TS sites by estimating the normal mode vibrational frequencies, which were estimated from the second derivative matrix, i.e., the Hessian, using a small displacement of 0.15 Å.

The kinetic rate constant for the individual hops (O-T or T-O) can be estimated using Eq. (4),[20,21]

$$k_{x-y}(\mathrm{NN},\mathrm{NNN},a) = \frac{\Pi_{i=1}^{3}\nu_{x,i}}{\Pi_{i=1}^{2}\nu_{\mathrm{TS},i}^{*}}\exp\left(-\frac{E_a(\mathrm{NN},\mathrm{NNN},a)-\varepsilon_{zp}(E_O)+\varepsilon_{zp}^{*}}{k_BT}\right), \quad (4)$$

where ν_i are the normal mode frequencies for the energy minimum at the O or T site and ν_j^* are the normal mode frequencies for the transition state, ε_{zp} is the zero-point energy of hydrogen at the energy minimum and ε_{zp}^* is the zero-point energy at the transition state, E_a is the activation energy barrier ($E_{TS}-E_T$) or ($E_{TS}-E_O$) for O-T or T-O hops, respectively, x-y represents either O-T or T-O hop, k_B is Boltzmann's constant, a is the lattice constant of the alloy, and T is the temperature of the system. The bracketed items (NN, NNN, and a) represent the independent variables which are used to model activation energy, binding energy, and the rate constant.

The PdAg or PdAu structure used to estimate the diffusion coefficient was simulated using 6234 Pd and Ag (or Pd and Au) atoms randomly distributed on an fcc lattice assembly, after which approximately 231 hydrogen atoms were placed on randomly selected O sites. An O site was selected as the starting position for the diffusion process since the experimental results as well as the molecular dynamics simulations of hydrogen in the Pd lattice indicated that the hydrogen atoms spend a significant time at the O site as compared to the T site. A random number generator with the input seed obtained from the millionth fraction of current time (seconds) was used for the kinetic Monte Carlo (KMC) simulations. Each T to O hop (T-TS-O) was accepted with a probability of 1, since the hydrogen bound to the O site represented a lower energy state than that bound to the T site. Each O-T hop was accepted with a probability of $2k_{OT}/k_{TO}$ or higher. This methodology was reported by Kamakoti and Sholl[4] and was used in this work as well. For each cell, the number of T sites was double that of O sites and was accounted for in the probability of hops from O-T sites. Regardless of the outcome of each attempted hop, the time was incremented by $1/(4Nk_{TO})$, where N is the total number of hydrogen atoms. The classical method of estimating the diffusion coefficient involves the measurement of the distance between each atom (at time $t=t_1$) from its starting position ($t=0$) and then averaging the distances of several atoms at a given time. This method, however, is limited due to errors associated with the edge effects caused by the lattice boundary. For instance, an atom near the edge will take additional time to cover the same distance that an atom from the center would take, leading to an overall decrease in the diffusion coefficient. One option for avoiding such an error is to remove the H atoms that reach the edge of the simulation cell. This limitation can be avoided by modifying the algorithm according to (a) a new technique called first passage and (b)

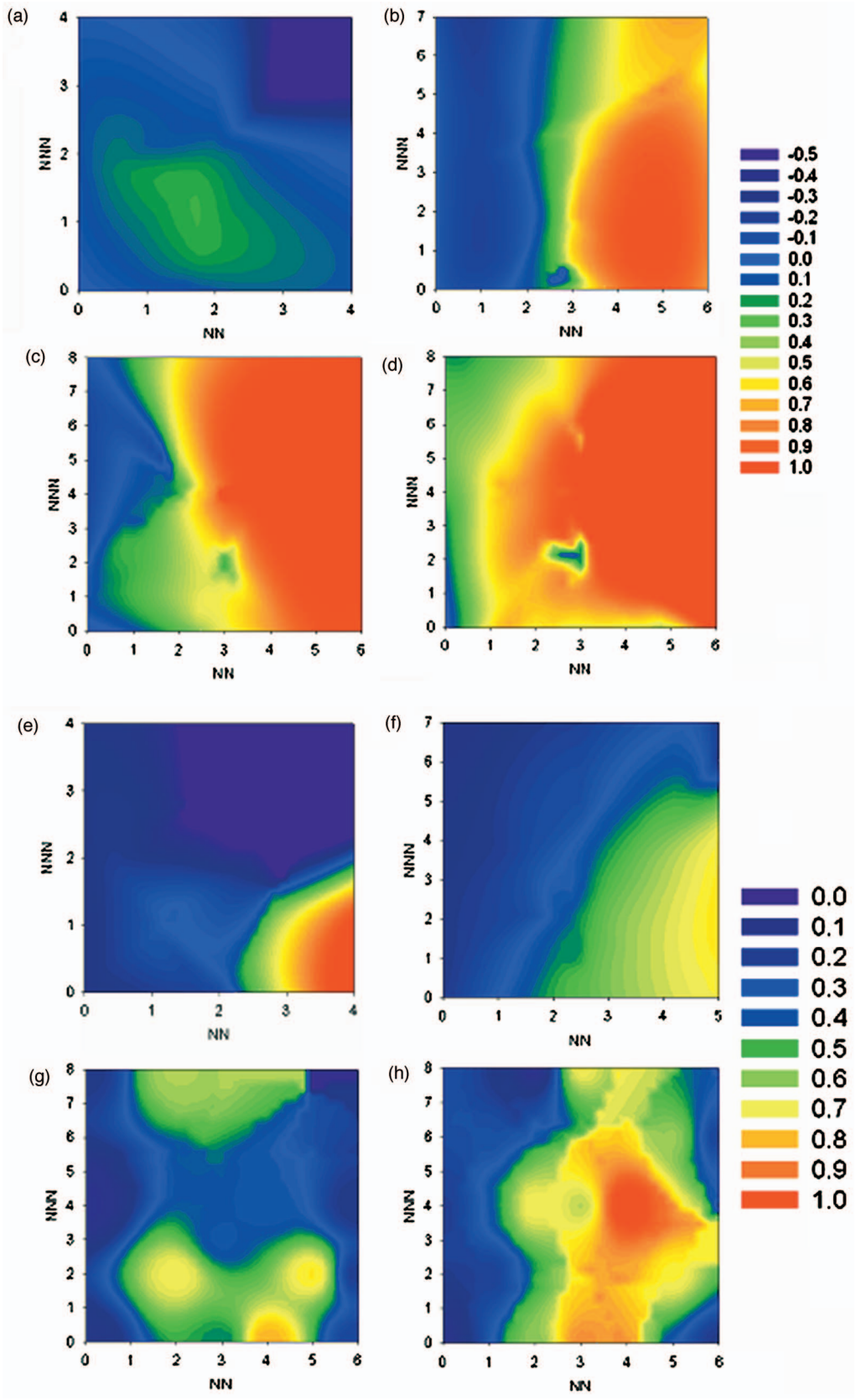

FIG. 1. (Color) TS-site energy of PdAg alloys: (a) 14.8%, (b) 25.9%, (c) 37.0%, and (d) 48.2%. Corresponding activation energies $E_{TS}-E_O$ for O-T hop are shown in (e), (f), (g), and (h), respectively.

by releasing the hydrogen atoms in a central spherical space. In the first passage method, the time required to cross a certain distance from the initial position for the first time is counted and used for the estimation of the diffusion coefficient. The diffusion coefficient was estimated using the Einstein equation as in (5),

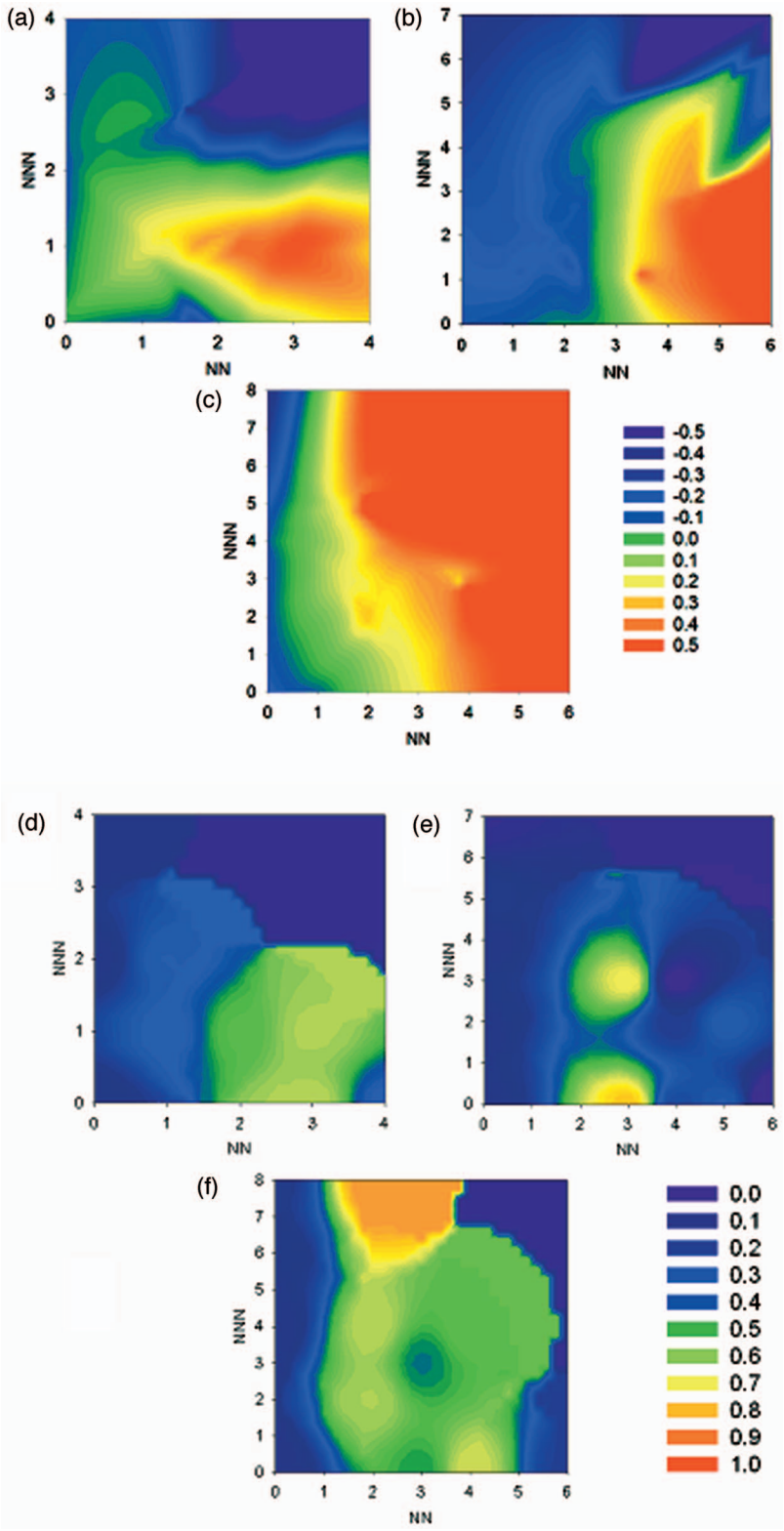

FIG. 2. (Color) TS-site energy of PdAu alloys: (a) 14.8%, (b) 25.9%, and (c) 37.0%. Corresponding activation energies $E_{TS}-E_O$ for O-T hop are shown in (d), (e), and (f), respectively.

$$D = \lim_{t\to\infty}\left[\frac{1}{6Nt}\sum_{i=1}^{N}\langle|R_i(t)-R_i(0)|^2\rangle\right], \tag{5}$$

where $R_i(t)$ is the position of an atom at time t and N is the number of H atoms used.

III. RESULTS AND DISCUSSION

A. Lattice constant of Pd–H system

The lattice constant of pure Pd obtained by DFT was found to be 3.96 Å, larger than the experimental value of 3.89 Å (Ref. 22) by 1.7% and close to the simulated value of 3.95 Å reported by Kamakoti *et al.*[2–4] In the past, the majority of simulations have ignored the expansion of the Pd lat-

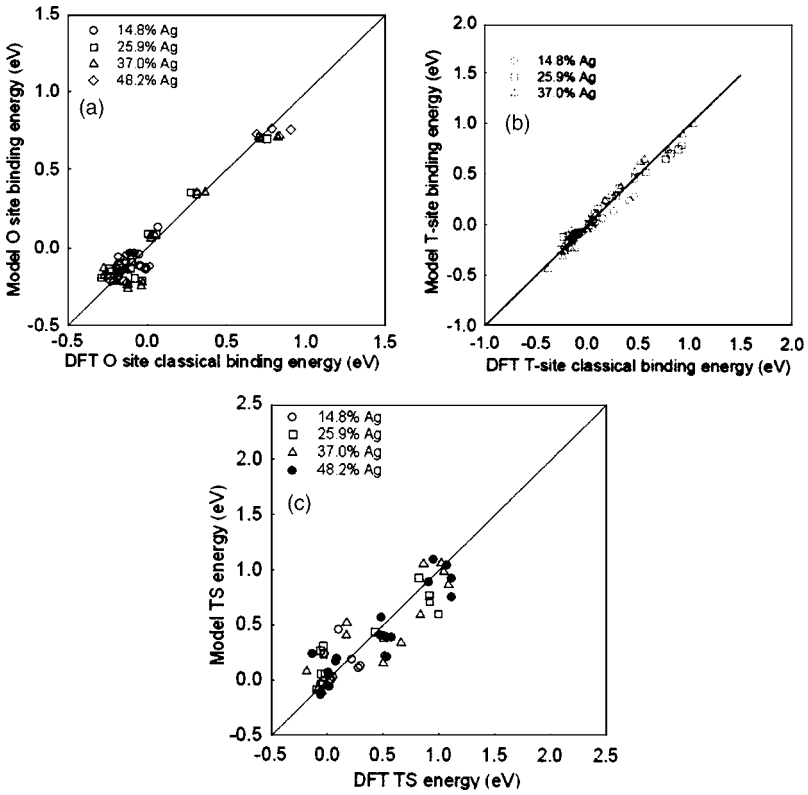

FIG. 3. Model and DFT based energy of O, T, and TS sites for PdAg alloy.

tice due to the addition of H by suggesting that it is negligible. Later, while discussing the binding energy and solubility predictions, it will be shown that even for a dilute concentration of H, i.e., 3.7% H in Pd alloys, the predicted binding energies are higher by 3.56% and eventually the solubility is underpredicted by about 11.8%.

B. O-, T-, and TS-site energy

The energetics of O, T, and TS sites (E_O, E_T, and E_{TS}) have been estimated as a function of local alloy composition. An H atom was placed at one O or T site with the number of nearest neighbors (NN_X) and next nearest neighbors (NNN_X) variable. For an O site, $0 \leqslant NN_O \leqslant 6$, $0 \leqslant NNN_O \leqslant 8$, and for a T site, $0 \leqslant NN_T \leqslant 4$ and $0 \leqslant NNN_T \leqslant 12$, which represent the possible values of alloying atom (Ag or Au), with the remainder of the nearest and next nearest atoms Pd.

The transition state energies of PdAg and PdAu alloys are shown in two-dimensional (2D) contour plots in Figs. 1 and 2, respectively. The binding energies, E_O and E_T, were

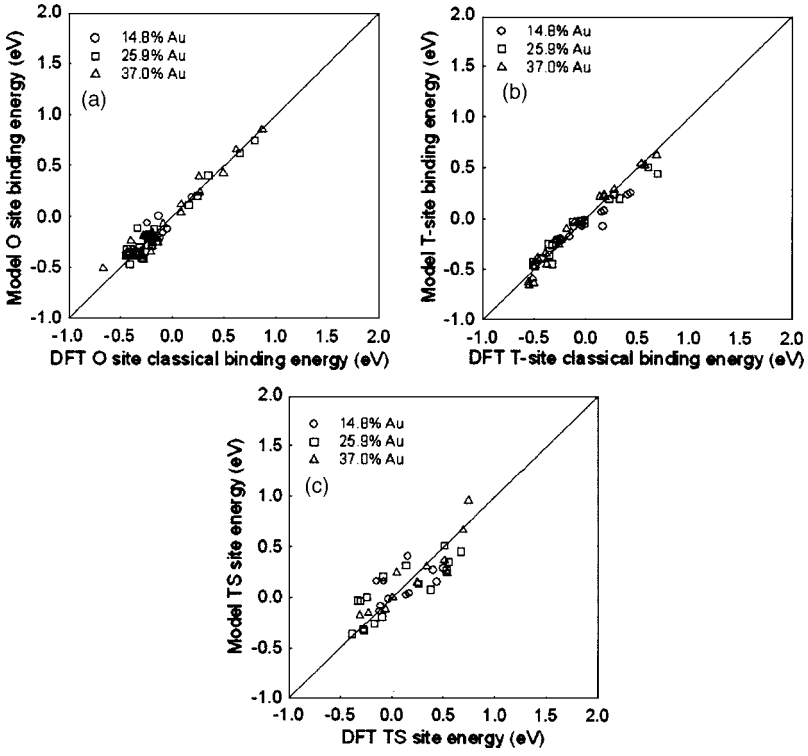

FIG. 4. Model and DFT based energy of O, T, and TS sites for PdAu alloy.

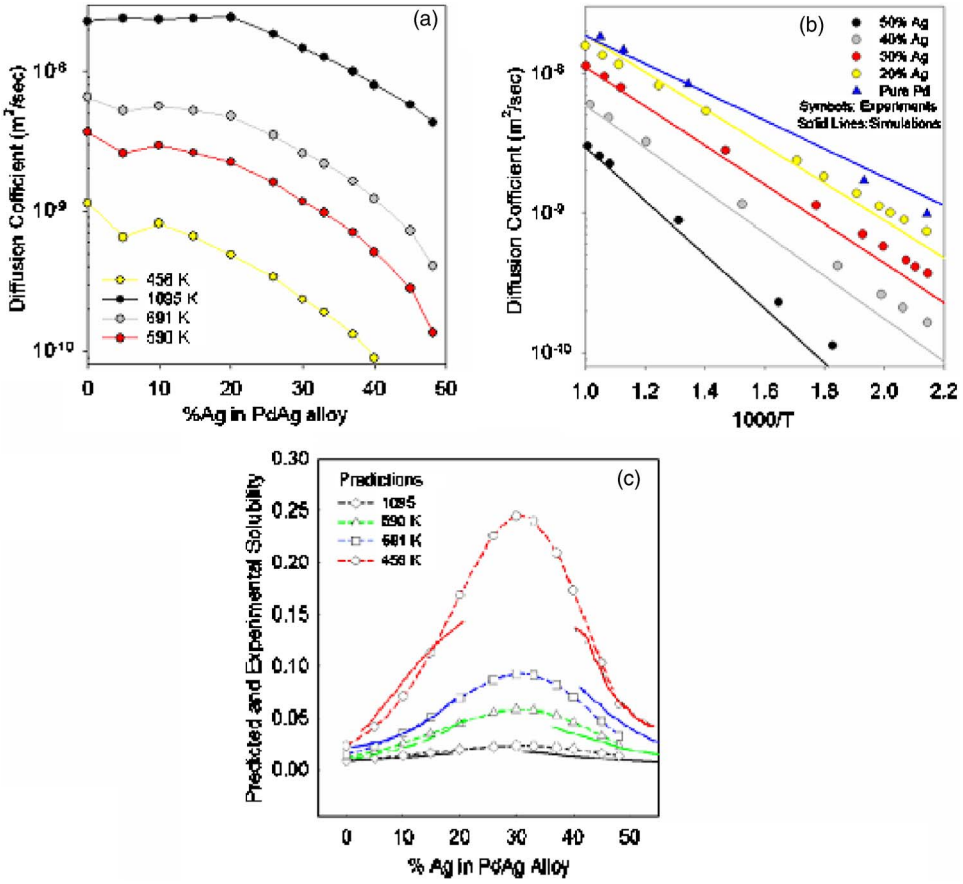

FIG. 5. [(a) and (b)] Diffusion coefficient and (c) solubility of PdAg alloy as a function of temperature and alloy composition.

calculated in a similar manner, with the details presented in an earlier manuscript.[23] The purpose of obtaining these TS plots is to show that the TS energy for an alloy is not constant, but rather, depends upon the local alloy composition. The NN_O and NNN_O for transition state energy plots represent the nearest neighbors and next nearest neighbors for the adjacent O site, respectively. The transition state energy can then be combined with the O-site binding energy to gain an understanding of the variation in activation energy (for an O-T hop) as a function of local alloy composition. A plot of activation energy ($E_{A,O}=E_{TS}-E_O$) for an O-T hop is plotted as a function of NN_O and NNN_O for each of the four alloys studied for PdAg as shown in Figs. 1(e)–1(h), as well as for PdAu alloys as shown in Fig. 2(d)–2(f). The activation energy $E_{A,O}$ fluctuates, and no overall trend can be found for its dependence upon NN_O and NNN_O. For a 14.8% Ag alloy, the maximum $E_{TS}-E_O$ value was found to be 1.14 eV ($NN_O=4$, $NNN_O=0$), with a minimum of 0.019 eV ($NN_O=2$, $NNN_O=2$). For the 25.9% Ag, corresponding values were 0.938 eV ($NN_O=4$, $NNN_O=2$) and 0.0.19 eV ($NN_O=2$, $NNN_O=5$). The 37.0% Ag yielded values of 0.79 eV ($NN_O=4$, $NNN_O=0$) and 0.055 eV ($NN_O=0$, $NNN_O=4$). For 48.2% Ag the maximum and minimum were 1.07 eV ($NN_O=4$, $NNN_O=4$) and 0.03 eV ($NN_O=2$, $NNN_O=8$), respectively. It can be observed that the maximum $E_{A,O}$ in most cases occurs at the higher NN_O sites and the lower NNN_O sites while the minimum $E_{A,O}$ occurs at the lower NN_O sites and the higher NNN_O sites.

For the purpose of gaining several O-, T-, and TS-site energies, a model was developed for representing the classical energies in a form that could be used to estimate the binding energy of any alloy in the 0%–50% Ag range of which individual O, T, and TS sites could be identified by means of local alloy composition (NN and NNN) and the lattice constant. The E_O, E_T, and E_{TS} energy data for all four PdAg and three PdAu alloys were combined to fit a nonlinear equation given by (6)

$$E_O = a_1 + a_2 n_{NN} + a_3 n_{NNN} + a_4 a_0 + a_5 n_{NN} n_{NNN} + a_6 n_{NN} a_0 + a_7 n_{NNN} a_0 + a_8 n_{NN}^2 + a_9 n_{NNN}^2 + a_{10} a_0^2, \quad (6)$$

where a_0 is the lattice constant, n_{NN} and n_{NNN} are the nearest and next nearest neighboring alloying atoms (Ag or Au), respectively, and a_1-a_{10} are fitting parameter constants for PdAg and PdAu. While using the equation, it should be noted that the NN and NNN for T and O sites, are unique. For instance, the O site and TS site have $0 \leqslant NN \leqslant 6$ and $0 \leqslant NNN \leqslant 8$, while the T site has $0 \leqslant NN \leqslant 4$ and $0 \leqslant NNN \leqslant 12$.

As discussed earlier, estimates of DFT-based O-, T-, and TS-site energies have been obtained from a single supercell for different alloy compositions to obtain a model O-site binding energy for a larger alloy. A comparison of model and classical O-, T-, and TS-site binding energies of PdAg and PdAu alloys are shown in Figs. 3(a)–3(c) and 4(a)–4(c), respectively.

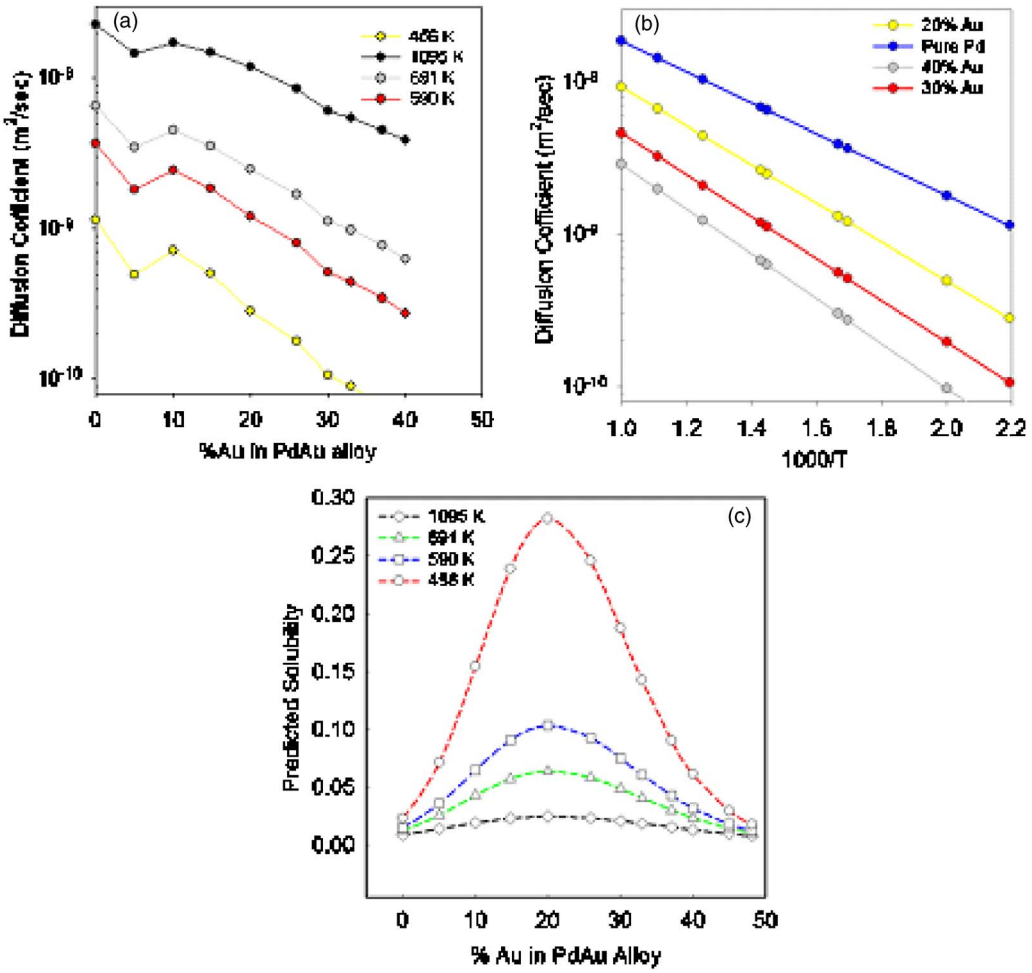

FIG. 6. [(a) and (b)] Diffusion coefficient and (c) solubility of PdAu alloy as a function of temperature and alloy composition.

C. Diffusion coefficient and permeability

The estimates of the diffusion coefficient D have been obtained in the present work for PdAg and PdAu alloys and are shown in Figs. 5 and 6, respectively. Estimates of D plotted in Fig. 5(a) show that for a given temperature, D decreases with increasing Ag content. Regardless of the alloying species, i.e., Ag or Au, D increases at approximately 5% Ag or Au content and proceeds to dip thereafter. It is not expected that this diffusion behavior occurs experimentally but is believed to be a limitation in the model at low concentrations of Ag and Au alloy content. For pure Pd, D at 456 K was found to be 1.146×10^{-9} m^2/s. More specifically, when the concentration is 5% Ag, D drops to 6.439×10^{-9} m^2/s and is followed by an increase of 8.178×10^{-9} m^2/s at 10% Ag. The diffusion coefficient decreases gradually with increasing Ag content and at 45% Ag, D is 4.34×10^{-11} m^2/s. A similar trend was observed at higher temperatures such as 590 and 691 K with the only difference being the drop in diffusion coefficient occurring at less than or equal to 5% Ag. At 1095 K, the diffusion coefficient remains almost constant over the Ag concentration of 0%–20% and decreases gradually thereafter. The comparison of our results with the experimental[23] data shows a close match at high temperature and a small error where the simulations underpredict the experiments at low temperatures. This could be due in part to the fact that the simulations involve a perfect lattice model, where as in reality, the lattice will experience grain boundary migration, which promotes hydrogen to diffusion through the lattice.

The diffusion coefficient of H in a PdAu alloy is shown in Fig. 6(a) and 6(b). Similar to PdAg alloys, the diffusion coefficient decreases with increasing Au content at a given temperature. Here too, a sudden decrease in the diffusion coefficient is observed at 5% Au with an increase at an Au composition of 10% and a gradual decrease at greater concentrations. At 456 K, D for 5% Au is 4.97×10^{-10} m^2/s, while for 10%, D is 7.133×10^{-10} m^2/s. The diffusion coefficient for 40% Au is 5.055×10^{-11} m^2/s. The diffusion coefficient of H in PdAg is higher than that in PdAu alloy.

A comparison of the solubilities of H in PdAg alloy at 456, 590, 691, and 1095 K for a broad range of alloy composition, i.e., from 0%–50% Ag is shown in Fig. 5(c). Our model overpredicts the solubility of H in a PdAg alloy at 456 K in the 20%–40% Ag range. However, for higher temperatures, i.e., 590, 691, or 1095 K, the predicted solubilities match closely with experimental data.[24] The predicted solubilities of H in PdAu alloys at 456, 590, 691, and 1095 K is shown in Fig. 6(c). It can be seen from Figs. 5(c) and 6(c) that the solubility of H in PdAg and PdAu alloys at a given temperature increases with increasing alloying metal concen-

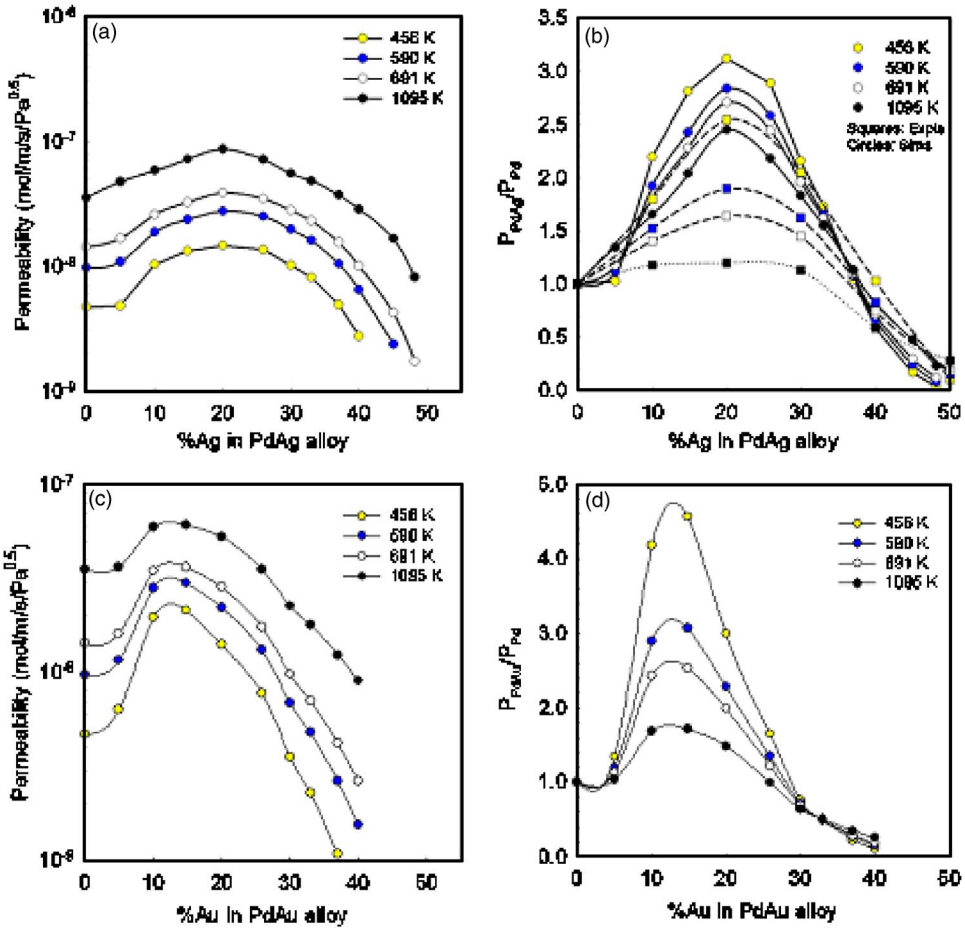

FIG. 7. (a) Permeability of PdAg alloy and (b) P_{Pd}/P_{PdAg}, experimental data taken from Holleck (1970) (Ref. 7), and (c) permeability of PdAu alloy and (d) P_{Pd}/P_{PdAu}.

tration (Ag or Au) and reaches a maximum and decreases thereafter. For example, the solubility of H in a PdAg alloy at 456 K and 30% Ag is about ten times higher than that of pure Pd. Similarly, the solubility at 590 K is six times higher than that of pure Pd. For other temperatures, i.e., 691 and 1095 K, the solubilities of H in the same alloy is five and three times higher than that of pure Pd, respectively. The maximum solubility was always found to occur around 30% Ag in PdAg alloys. The solubility of PdAu alloys shown in Fig. 6(c) also exhibits a similar trend, except that the solubility for the given temperature and composition is higher than the PdAg system and with the maximum solubility occurring at approximately 20% Au content. The solubility of H at 456 K in PdAu with 20% Au is about 12 times higher than that of pure Pd. Comparing this with the corresponding PdAg system with solubility ten times higher than that of pure Pd, the maximum solubilities for PdAu at 590, 691, and 1095 K are seven, five, and three times higher than that of pure Pd, respectively.

The diffusion coefficient and solubility estimates were then combined to obtain the H permeabilities as shown in Fig. 7. The absolute values of permeability as a function of % Ag for various temperatures is shown in Fig. 7(a), while the ratio of PdAg alloy permeability to that of pure Pd at various temperatures is shown in Fig. 7(b). Similar plots for PdAu are shown in Fig. 7(c) and 7(d). It can be seen that the permeability of H increases with increasing Ag content until it reaches ~20% at which point it decreases. The H permeability in pure Pd at 456 K is 4.713×10^{-9}, while in 20% Ag it is 1.46×10^{-8}, which implies that the permeability in PdAg is three times greater than pure Pd at this temperature and composition. Going from pure Pd to 5% Ag, there is no significant increase in permeability at low temperatures for PdAg alloy. However, with an increase in temperature, the ratio R of PdAg to Pd at 20% Ag decreases. At higher temperatures, i.e., 1095 K, the permeability is significantly high at 8.6879×10^{-8}, but the ratio of its permeability to that of pure Pd is just 2.45. After about 38% Ag content, the permeability of PdAg alloy at all temperatures is lower than the pure Pd at the same temperature.

The permeability of PdAu as a function of alloy composition at various temperatures shows minimal variance. At low temperatures, in going from pure Pd to 5% Au, the permeability increases at low temperatures, i.e., 456 K, but almost remains constant at high temperatures, i.e., 1095 K. The permeability of H in 5% Au at 456 K is 6.3437×10^{-9} as compared to 4.7131×10^{-9} for pure Pd. The values at 1095 K are 3.5448×10^{-8} (pure Pd) and 3.6533×10^{-8} (5% Au). The permeability of H in PdAu increases with increasing Au content until it reaches ~12% Au concentration and decreases thereafter. The permeability of H at 456 K in 12% Au content is about 4.8 times that of pure Pd. This ratio is higher than the PdAg alloy for which we found it to be 3.1 times greater at 20% Ag content. At concentrations between 25% and 30% Au, the permeability is lower than that of pure Pd.

The permeability predictions for PdAg are compared to experimental data in Fig. 7(b). The theoretical predictions are accurate in terms of predicting the alloy composition that yields the maximum hydrogen permeability but is not as accurate in matching directly the experimental permeability. This could be caused from the cumulative error associated with the solubility and diffusivity predictions. Although examination of each of these parameters separately yields minimal deviation from experiment for the theoretical predictions, when combined to obtain the permeability, the deviation from experiment is compounded.

The present work reveals that a simulation method can be used to design a highly permeable membrane for efficient H separation. The concentration of alloying atom and the temperature can be adjusted to maximize H permeability.

IV. CONCLUSIONS

In the present work, diffusion coefficients have been estimated for H transport through PdAg and PdAu alloys over a broad range of temperatures and compositions. The estimates of diffusion coefficients were then combined with solubility predictions to estimate the permeability of H through PdAg and PdAu alloys. Rate constants were estimated for individual hops throughout the lattice, and corresponding activation energies were used in kinetic Monte Carlo simulations by applying the first passage method to the diffusion coefficient estimate. It was found that the H diffusion coefficient in PdAg alloy decreases with either decreasing temperature or increasing Ag content, matching closely with the experimental results reported in the literature. Similar results were obtained for the PdAu alloys. The H permeability in PdAg and PdAu alloys was found to increase with increasing Ag (and Au) showing a maximum at ~20% Ag (and ~12% Au for PdAu alloy). The permeability of H in 20% Ag PdAg alloy at 456 K is three to four times higher than pure Pd, while 12% Au PdAu alloy yields a permeability 1.8 times greater than pure Pd.

ACKNOWLEDGMENTS

We acknowledge the Shell International Exploration and Production Company Inc. and Shell Hydrogen for financial support and Mr. Josh Brandt with assistance in computational resources and support.

[1] W. Wicke and H. Brodowsky, in *Hydrogen in Metals 2*, edited by G. Alefeld and J. Volkl (Springer-Verlag, Berlin, 1978), p. 73.
[2] P. Kamakoti, B. D. Morreale, M. V. Ciocco, B. H. Howard, R. P. Killmeyer, A. V. Cugini, and D. S. Sholl, Science **307**, 569 (2005).
[3] P. Kamakoti and D. S. Sholl, J. Membr. Sci. **225**, 145 (2003).
[4] P. Kamakoti and D. S. Sholl, Phys. Rev. B **71**, 014301-1 (2005).
[5] T. Graham, Proc. R. Soc. London **17**, 212 (1869).
[6] V. M. Gryaznov, Sep. Purif. Methods **29**, 171 (2000).
[7] G. L. Holleck, J. Phys. Chem. **74**, 503 (1970).
[8] S. Uemiya, T. Matsuda, and E. Kikuchi, J. Membr. Sci. **56**, 315 (1991).
[9] H. Amandusson, L.-G. Ekedahl, and H. Dannetun, J. Membr. Sci. **193**, 35 (2001).
[10] Y. Yokoi, T. Seki, and I. Yasuda, in *Advances in H Energy*, edited by G. Padro and E. Catherine (Kluwer, Dordrecht, 2000), p. 111.
[11] X. Ke and G. J. Kramer, Phys. Rev. B **66**, 184304 (2002).
[12] O. M. Løvvik and R. A. Olsen, J. Alloys Compd. **330–332**, 332 (2002).
[13] G. Kresse and J. Hafner, Phys. Rev. B **48**, 13115 (1993).
[14] G. Kresse and J. Furthmuller, Comput. Mater. Sci. **6**, 15 (1996).
[15] *Binary Alloy Phase Diagram*, edited by T. B. Massalski (American Society for Metals, Metals Park, OH, 1986), Vols. 1 & 2.
[16] R. H. Fowler and C. J. Smithells, Proc. R. Soc. London, Ser. A **160** 900, 900 (1937).
[17] C. Wagner, Acta Metall. **21**, 1297 (1973).
[18] R. Malek and N. Mousseau, Phys. Rev. E **62**, 7723 (2000).
[19] G. Henkelman and H. Jonsson, J. Chem. Phys. **111**, 7010 (1999).
[20] J. Volkl and G. Alefield, in *Hydrogen in Metals I*, edited by G. Alefield and J. Volkl (Springer, Berlin, 1978), Vol. 28, p. 321.
[21] K. Haug and T. Jenkins, J. Phys. Chem. B **104**, 10017 (2000).
[22] W. B. Pearson, *A Handbook of Lattice Spacing and Structure of Metal and Alloys* (Pergamon, New York, 1967), Vol. 2.
[23] S. Sonwane, J. Wilcox, and Y. H. Ma, J. Phys. Chem. B (in press).
[24] A. G. Knapton, Platinum Met. Rev. **21**, 44 (1977).